Available online at www.sciencedirect.com
SCIENCE DIRECT®
ELSEVIER
International Journal of Heat and Mass Transfer 49 (2006) 329–340
International Journal of HEAT and MASS TRANSFER
www.elsevier.com/locate/ijhmt

Regenerative heat exchangers with significant entrained fluid heat capacity

Gregory F. Nellis *, Sanford A. Klein

University of Wisconsin, 1500 Engineering Drive, Madison, WI 53706, USA

Received 12 December 2004; received in revised form 22 June 2005
Available online 25 August 2005

Abstract

Entrained fluid heat capacity is shown to have a significant and positive effect on the performance of a passive regenerator. The ineffectiveness of the regenerator is presented as a function of three dimensionless parameters: the number of transfer units, the utilization, and the entrained fluid to matrix heat capacity ratio. Three different behaviors are observed for a regenerator with entrained fluid heat capacity. The effect of the entrained fluid can be accounted for over a large range of conditions using the concept of an augmented-NTU which can be substituted for the actual NTU in analyses that neglect entrained fluid capacity.

Keywords: Regenerator; Entrained fluid; Modeling; Heat exchanger; Augmented NTU

1. Introduction

Regenerative heat exchangers are used in many applications including cryogenic refrigeration systems, for building energy recovery, and in gas turbine systems. The heat capacity of the fluid, often a gas that is entrained in the void volume of the regenerator matrix, is typically very small relative to the heat capacity associated with the regenerator matrix itself. Therefore, the effect of this entrained fluid heat capacity is almost always neglected in regenerator analyses. A large number of analytical and numerical solutions to the regenerator governing equations have been presented. These include papers by Nusselt [1], Hill and Wilmott [2], and Atthey [3] in which axial conduction is neglected, as well as works by Bahnke and Howard [4], Shen and Worek [5], and Klein and Eigenberger [6] which account for axial conduction. None of these analyses consider the effect of the entrained heat capacity in the regenerator.

Recently there has been considerable interest in active magnetic regenerative refrigeration (AMRR) systems for near room temperature applications [7–9]. In an AMRR system, a heat transfer fluid (e.g., water) is cyclically passed through a regenerator matrix that exhibits a magnetocaloric effect; the entropy of the matrix is affected by magnetic field as well as by temperature. The heat capacity of the fluid entrained in the matrix is non-negligible in this application and can be nearly equal to the matrix heat capacity in a practical design. As a result, the entrained fluid heat capacity should not be neglected when modeling an AMRR system. Also, regenerative heat exchangers are being used at increasingly lower temperatures in cryogenic refrigeration devices. At very low temperature, the volumetric

* Corresponding author. Tel.: +1 608 265 6266.
E-mail address: gfnellis@engr.wisc.edu (G.F. Nellis).

0017-9310/$ - see front matter © 2005 Elsevier Ltd. All rights reserved.
doi:10.1016/j.ijheatmasstransfer.2005.06.021

Nomenclature

A_s	surface area (m^2)
AF	augmentation factor
c	specific heat capacity (J/kg K)
C	total heat capacity (J/K)
CSR	critical time step ratio
h	heat transfer coefficient (W/m^2 K)
ieff	ineffectiveness
L	regenerator length (m)
$\dot{m}$	mass flow rate (kg/s)
n	number of control volumes in numerical solution
NTU	number of transfer units
NTU*	augmented number of transfer units
R	entrained fluid to regenerator capacity ratio
t	time (s)
T	temperature (K)
U	utilization
x	axial position (m)

Greek symbols

$\Delta\eta$	reduced time step
ε	effectiveness
η	reduced time
λ	duration of flow process (s)
Π	reduced period
θ	dimensionless temperature
ξ	reduced position

Subscripts

c	cold end of bed
cr	critical reduced time step
f	fluid
h	hot end of bed
i	subscript of control volume
r	regenerator

heat capacity of the entrained fluid increases due to its increasing density whereas the heat capacity of most solids rapidly decrease; therefore, the heat capacity of the entrained fluid may become non-negligible in this application.

There has been relatively little work that is aimed specifically at understanding the effect of entrained fluid heat capacity on regenerator performance. Willmott and Hinchcliffe [10] develop an approximate model that is used to estimate the effect of the entrained fluid heat capacity on the regenerator performance. They report results over a limited range of operating conditions and show that entrained gas has a generally positive effect on the performance of the regenerator, particularly when the number of transfer units is low. Daney and Radebaugh [11] numerically solve the governing equations for a matrix with entrained heat capacity and present a numerical experiment which demonstrates that, for low thermal loads, the effectiveness of the regenerator will actually decrease as the matrix heat capacity increases. They attribute this counter-intuitive behavior to the situation where a thermal wave is contained within the heat exchanger, a result that is consistent with the conclusions described here. Neither of these studies resulted in a complete understanding of how entrained heat capacity affects the performance of a passive regenerator, when the effect of entrained heat capacity is important, or how a designer might estimate the magnitude of this effect during a regenerator analysis.

This paper describes a numerical model in which the entrained heat capacity in a regenerator is included in the governing equations. The model is verified against solutions found in the literature in the limit of no entrained heat capacity and subsequently used to specifically investigate the behavior of a regenerator as the entrained heat capacity becomes significant. Three fundamental behaviors are identified: the ‘‘NTU-limited’’ and ‘‘capacity-limited’’ behaviors are found even in the absence of entrained fluid heat capacity; however, a third, ‘‘stratified’’ behavior is also observed. The behavior of the regenerator in this region is non-intuitive; performance may decrease with increasing NTU or increasing matrix heat capacity. The regimes associated with these behaviors are delineated on a map that is presented in terms of the fundamental dimensionless parameters that define the operating condition for the regenerator. The concept of an augmented-NTU is introduced to account for entrained fluid heat capacity in the ‘‘NTU-limited’’ region, which is the region of greatest practical interest to a regenerator designer. Using the augmented-NTU in place of the actual NTU allows computationally simpler models that neglect the effect of entrained fluid to provide estimates of regenerator performance that account for this effect. The augmented-NTU approach can be used in conjunction with other correction factors such as those proposed by Jeffreson to account for temperature gradients that are internal to the regenerator matrix and axial dispersion [12].

2. Governing equations

The governing equations for the regenerator are derived here assuming a passive regenerator with constant matrix and fluid properties, no axial conduction, and balanced flow. The purpose of this analysis is to specifically consider the effect of the entrained fluid heat capacity. One outcome of this work is an approximate correction technique, the augmented-NTU approach. Therefore, these assumptions are not particularly limiting as the authors expect that the concept of an augmented-NTU can be integrated with complex models of regenerative heat exchangers in much the same way that the Jeffreson correction is used.

The governing equation for the matrix is:

$$hA_s(T_f - T_r) = C_r \frac{\partial T_r}{\partial t} \tag{1}$$

where h is the heat transfer coefficient, A_s is the total surface area, C_r is the total regenerator heat capacity, T_f and T_r are the fluid and regenerator temperatures, and t is time. The flow pattern considered here consists of two processes. During the hot-to-cold flow process, a constant mass flow rate enters the matrix from the hot end ($x = 0$). During the cold-to-hot flow process, an equal mass flow rate enters the matrix from the cold end ($x = L$). The duration of the two processes (λ) is the same. The fluid energy balance during the hot-to-cold flow portion of the cycle ($0 < t < \lambda$) is:

$$\frac{hA_s}{L}(T_r - T_f) = \dot{m}c_f \frac{\partial T_f}{\partial x} + \frac{C_f}{L}\frac{\partial T_f}{\partial t} \tag{2}$$

where L is the length of the regenerator, $\dot{m}$ is the mass flow rate, c_f is the specific heat capacity of the fluid, and C_f is the total fluid heat capacity entrained in the regenerator. During the cold-to-hot flow portion of the cycle ($\lambda < t < 2\lambda$) the fluid energy balance becomes:

$$\frac{hA_s}{L}(T_r - T_f) + \dot{m}c_f \frac{\partial T_f}{\partial x} = \frac{C_f}{L}\frac{\partial T_f}{\partial t} \tag{3}$$

The inlet temperature of the fluid during the two flow processes is assumed to be constant in time:

$$T_f(x = 0, t) = T_h \quad 0 < t < \lambda \tag{4}$$

$$T_f(x = L, t) = T_c \quad \lambda < t < 2\lambda \tag{5}$$

where T_h is the hot end temperature and T_c is the cold end temperature. After initial transients have dissipated, the fluid and regenerator temperatures must go through a steady state cycle:

$$T_f(x, t = 0) = T_f(x, t = 2\lambda) \tag{6}$$

$$T_r(x, t = 0) = T_r(x, t = 2\lambda) \tag{7}$$

These equations are made dimensionless by defining a reduced position (ξ) and reduced time (η), as described by Ackerman [13]:

$$\xi = \frac{hA_s}{\dot{m}c_f}\frac{x}{L} \tag{8}$$

$$\eta = \frac{hA_s}{C_r} t \tag{9}$$

The dimensionless temperature (θ) is defined according to:

$$\theta = \frac{T - T_c}{T_h - T_c} \tag{10}$$

The reduced period (Π) and number of transfer units (NTU) are defined according to:

$$\Pi = \frac{hA_s}{C_r}\lambda \tag{11}$$

$$\mathrm{NTU} = \frac{hA_s}{\dot{m}c_f} \tag{12}$$

Finally, the entrained fluid to regenerator capacity ratio (R) is defined:

$$R = \frac{C_f}{C_r} \tag{13}$$

Substituting Eqs. (8)–(13) into Eqs. (1)–(7) leads to:

$$\frac{\partial \theta_r}{\partial \eta} = \theta_f - \theta_r \tag{14}$$

$$\frac{\partial \theta_f}{\partial \xi} + R\frac{\partial \theta_f}{\partial \eta} = \theta_r - \theta_f \quad 0 < \eta < \Pi \tag{15}$$

$$\frac{\partial \theta_f}{\partial \xi} = R\frac{\partial \theta_f}{\partial \eta} + \theta_f - \theta_r \quad \Pi < \eta < 2\Pi \tag{16}$$

The boundary conditions are:

$$\theta_f(\xi = 0, \eta) = 1 \quad 0 < \eta < \Pi \tag{17}$$

$$\theta_f(\xi = \mathrm{NTU}, \eta) = 0 \quad \Pi < \eta < 2\Pi \tag{18}$$

$$\theta_f(\xi, \eta = 0) = \theta_f(\xi, \eta = 2\Pi) \tag{19}$$

$$\theta_r(\xi, \eta = 0) = \theta_r(\xi, \eta = 2\Pi) \tag{20}$$

The effectiveness of the regenerator (ε) is defined as:

$$\varepsilon = \frac{\int_0^\lambda [T_w - T_f(x = L, t)]\mathrm{d}t}{[T_w - T_c]\lambda} \tag{21}$$

or

$$\varepsilon = \frac{1}{\Pi}\int_0^\Pi [1 - \theta_f(\xi = \mathrm{NTU}, \eta)]\mathrm{d}\eta \tag{22}$$

The ineffectiveness (ieff) is therefore:

$$\mathrm{ieff} = 1 - \varepsilon = \frac{1}{\Pi}\int_0^\Pi \theta_f(\xi = \mathrm{NTU}, \eta)\,\mathrm{d}\eta \tag{23}$$

3. Numerical solution

The governing equations are solved in the general limit where R is finite and non-zero as well as in the specific limit where R is zero, corresponding to no fluid heat capacity entrained in the matrix. In either case, the solution is obtained over a uniformly distributed set of n control volumes such that:

$$\xi_i = \frac{(i - 0.5)}{n}\mathrm{NTU} \quad i = 1, \ldots, n \tag{24}$$

The discretized form of Eq. (14) provides the time rate of change of the dimensionless regenerator temperature for any control volume:

$$\left(\frac{\partial\theta_r}{\partial\eta}\right)_i = \theta_{f,i} - \theta_{r,i} \quad \text{for } i = 1,\ldots,n \tag{25}$$

If R is finite, then the time rate of change of the dimensionless fluid temperature for an internal control volume is obtained by discretizing Eqs. (15) and (16):

$$\left(\frac{\partial\theta_f}{\partial\eta}\right)_i = \frac{1}{R}\left[\theta_{r,i} - \theta_{f,i} - \frac{(\theta_{f,i+1} - \theta_{f,i-1})n}{2\text{NTU}}\right] \quad i = 2,\ldots,(n-1)\ 0 < \eta < \Pi \tag{26}$$

$$\left(\frac{\partial\theta_f}{\partial\eta}\right)_i = \frac{1}{R}\left[\theta_{r,i} - \theta_{f,i} + \frac{(\theta_{f,i+1} - \theta_{f,i-1})n}{2\text{NTU}}\right] \quad i = 2,\ldots,(n-1)\ 0 < \eta < \Pi \tag{27}$$

For the control volumes at the edges of the computational domain, the discretized form of Eqs. (26) and (27) for the control volumes that are adjacent to the hot end and cold end are:

$$\left(\frac{\partial\theta_f}{\partial\eta}\right)_1 = \frac{1}{R}\left[\theta_{r,1} - \theta_{f,1} - \frac{(\theta_{f,2} - 1)2n}{3\text{NTU}}\right] \quad 0 < \eta < \Pi \tag{28}$$

$$\left(\frac{\partial\theta_f}{\partial\eta}\right)_1 = \frac{1}{R}\left[\theta_{r,1} - \theta_{f,1} + \frac{(\theta_{f,2} - \theta_{f,1})n}{\text{NTU}}\right] \quad \Pi < \eta < 2\Pi \tag{29}$$

$$\left(\frac{\partial\theta_f}{\partial\eta}\right)_n = \frac{1}{R}\left[\theta_{r,n} - \theta_{f,n} - \frac{(\theta_{f,n} - \theta_{f,n-1})n}{\text{NTU}}\right] \quad 0 < \eta < \Pi \tag{30}$$

$$\left(\frac{\partial\theta_f}{\partial\eta}\right)_n = \frac{1}{R}\left[\theta_{r,n} - \theta_{f,n} + \frac{(0 - \theta_{f,n-1})2n}{3\text{NTU}}\right] \quad \Pi < \eta < 2\Pi \tag{31}$$

Eqs. (25)–(31) are integrated forward in time using a predictor–corrector technique until a cyclic steady state is achieved. A cyclic steady state is defined based on the relative change in the ineffectiveness calculated using Eq. (23), between subsequent cycles. For the cases reported in this paper, a cyclic steady state occurs when the relative change in ineffectiveness is less than 0.001%.

The size of the reduced time step ($\Delta\eta$) used to carry out the time integration is based on an estimate of the critical reduced time step required for numerical stability ($\Delta\eta_{cr}$). Evaluating Eq. (29) for the critical time step yields:

$$\Delta\eta_{cr} = \frac{R}{1 + \frac{n}{\text{NTU}}} \tag{32}$$

The reduced timestep used in the simulation is specified as a ratio of this critical reduced timestep (CSR):

$$\Delta\eta = \text{CSR}\,\Delta\eta_{cr} \tag{33}$$

The value of CSR used for the results reported here is 0.05 and the number of control volumes, n, is 800. Sensitivity studies indicated that these numerical parameters provided ineffectiveness values that were accurate to at least 0.0001 over most conditions.

In the limit of R equal to zero, the governing equations change fundamentally; the rate of change of the dimensionless fluid temperature is unbounded in this limit according to Eqs. (26)–(31). Alternatively, Eq. (32) shows that an infinitely small time step is required for stability as R approaches zero. In this limit, the dimensionless fluid temperature distribution responds instantly to changes in the dimensionless regenerator temperature distribution. The system of equations that defines the dimensionless fluid temperatures at each time step is:

$$\theta_{r,i} - \theta_{f,i} - \frac{(\theta_{f,i+1} - \theta_{f,i-1})n}{2\text{NTU}} = 0 \quad i = 2,\ldots,(n-1)\ 0 < \eta < \Pi \tag{34}$$

$$\theta_{r,i} - \theta_{f,i} + \frac{(\theta_{f,i+1} - \theta_{f,i-1})n}{2\text{NTU}} = 0 \quad i = 2,\ldots,(n-1)\ 0 < \eta < \Pi \tag{35}$$

$$\theta_{r,1} - \theta_{f,1} - \frac{(\theta_{f,2} - 1)2n}{3\text{NTU}} = 0 \quad 0 < \eta < \Pi \tag{36}$$

$$\theta_{r,1} - \theta_{f,1} + \frac{(\theta_{f,2} - \theta_{f,1})n}{\text{NTU}} = 0 \quad \Pi < \eta < 2\Pi \tag{37}$$

$$\theta_{r,n} - \theta_{f,n} - \frac{(\theta_{f,n} - \theta_{f,n-1})n}{\text{NTU}} = 0 \quad 0 < \eta < \Pi \tag{38}$$

$$\theta_{r,n} - \theta_{f,n} + \frac{(0 - \theta_{f,n-1})2n}{3\text{NTU}} = 0 \quad \Pi < \eta < 2\Pi \tag{39}$$

The dimensionless regenerator temperatures are integrated forward in time using Eq. (25) with the same predictor–corrector technique. The dimensionless fluid temperatures at each time are calculated using Eqs. (34)–(39) and the process is continued until a cyclic steady state is reached.

4. Verification of model

The ineffectiveness of the regenerator is a function of three dimensionless variables: the number of transfer units, reduced period, and the entrained fluid to regenerator capacity ratio:

$$\text{ieff} = \text{ieff}(\text{NTU}, \Pi, R) \tag{40}$$

A dimensionless parameter that is more physically meaningful than the reduced period (Π) is the utilization (U) which is the ratio of the heat capacity of the fluid forced through the regenerator to the total heat capacity in the regenerator. Here, the utilization is defined based on the sum of the heat capacity of the entrained fluid and the regenerator matrix.

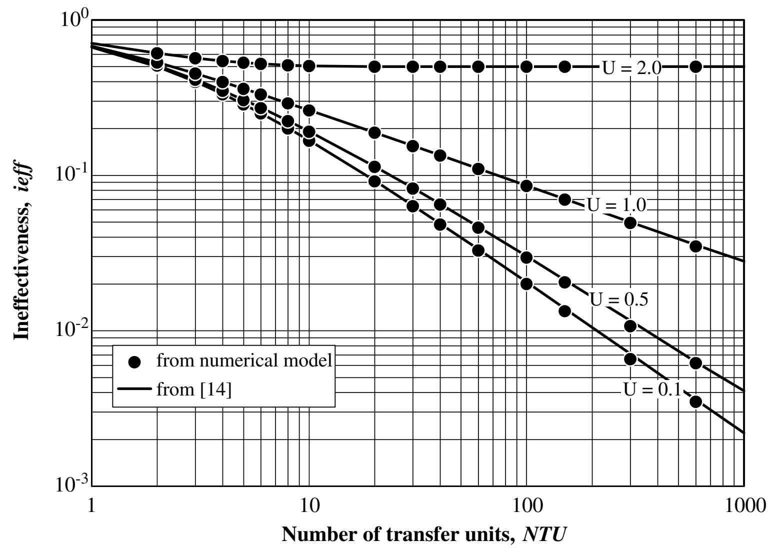

Fig. 1. Ineffectiveness as a function of NTU for different values of U in the $R = 0$ limit.

$$U = \frac{\dot{m}c_f\lambda}{(C_r + C_f)} = \frac{\Pi}{NTU(1+R)} \tag{41}$$

The functional form of the ineffectiveness can therefore be written as:

$$\text{ieff} = \text{ieff}(\text{NTU}, U, R) \tag{42}$$

In the limit of zero entrained fluid heat capacity ($R = 0$) it is possible to compare the results of this model with results reported in the literature. For example, Dragutinovic and Baclic [14] tabulate the ineffectiveness of a balanced and symmetric regenerator as a function of U and NTU. Fig. 1 illustrates the ineffectiveness predicted by the numerical model presented here in the $R = 0$ limit as a function of NTU for several values of U. Also shown are the results presented in [14]. Note the good agreement over a wide range of U and NTU.

5. Results

Fig. 2 illustrates the ineffectiveness of the regenerator as a function of NTU for $U = 0.1$ and two values of R:

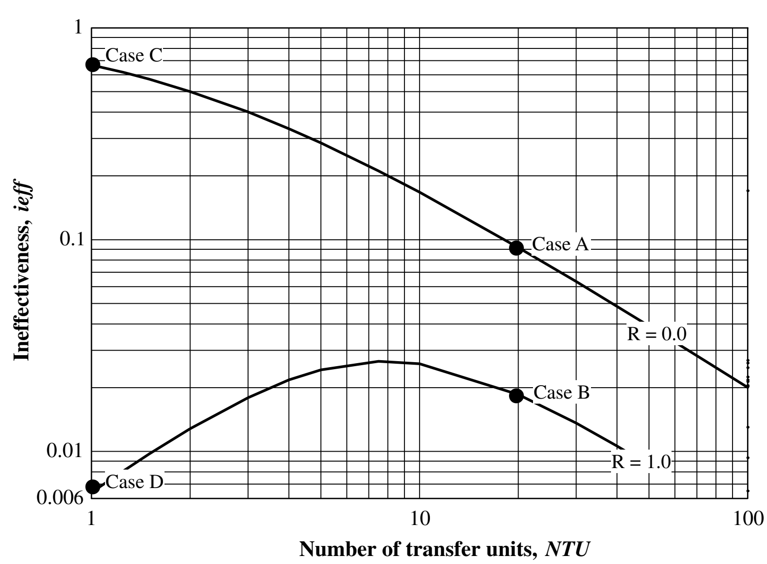

Fig. 2. Ineffectiveness as a function of NTU for $U = 0.1$, a regenerator in which the total heat capacity is $10\times$ the capacity of the flowing fluid capacity with $R = 0.0$ (all capacity in the matrix) and $R = 1.0$ (capacity split equally between matrix and entrained fluid).

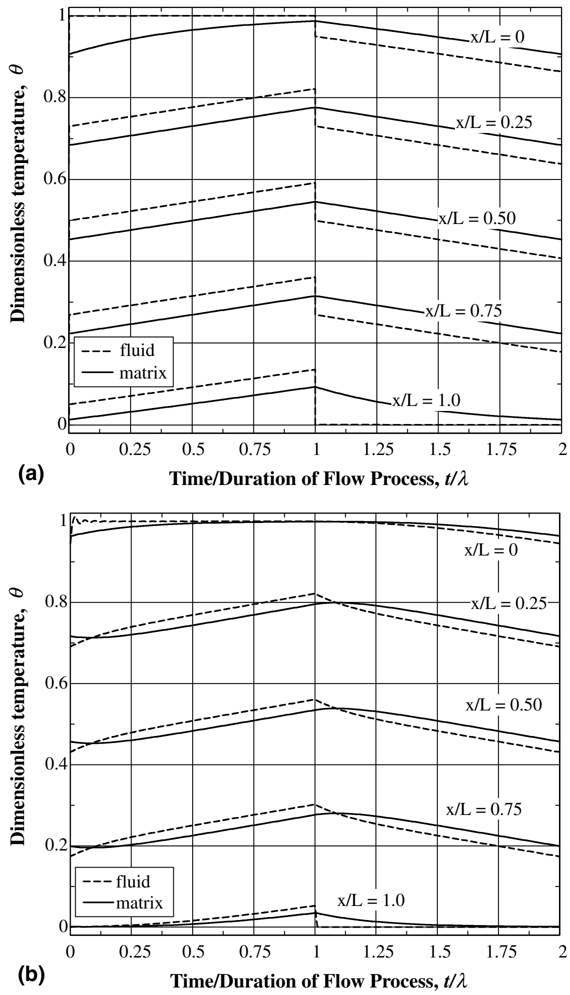

Fig. 3. Dimensionless temperature as a function of dimensionless time at several axial locations for (a) Case A: NTU = 20, $U = 0.1$, and $R = 0.0$, and (b) Case B: NTU = 20, $U = 0.1$, and $R = 1.0$.

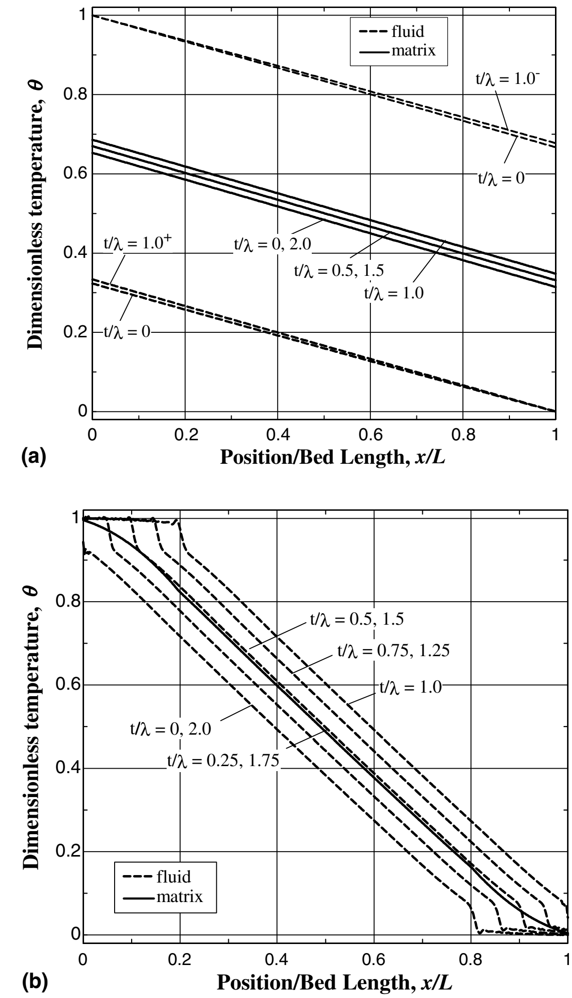

Fig. 4. Dimensionless temperature as a function of dimensionless axial position at several times for (a) Case C: NTU = 1.0, $U = 0.1$, and $R = 0.0$, and (b) Case D: NTU = 1.0, $U = 0.1$, and $R = 1.0$.

$R = 0$ and $R = 1.0$. The curves correspond to two regenerators that have the same total heat capacity which is large relative to the heat capacity of the flowing fluid; in the $R = 0$ case this heat capacity is entirely in the matrix whereas in the $R = 1.0$ case, the heat capacity is split equally between the matrix and the entrained fluid. At any value of NTU, the regenerator performance is improved as R is increased from 0 to 1. However, regenerator performance exhibits a non-intuitive dependence on NTU at $R = 1$, first decreasing and then increasing, as NTU is increased.

A general observation, seen in Fig. 2, is that the performance of the regenerator is always enhanced when more of the total available heat capacity is associated with the fluid as opposed to the regenerator, i.e., as R is increased. Increasing R essentially removes the resistance to heat transfer between the fluid and some of the available heat capacity that is otherwise associated with the fluid-to-matrix heat transfer coefficient.

Fig. 3(a) illustrates the dimensionless temperature as a function of dimensionless time for NTU = 20, $U = 0.1$, and $R = 0$ (Case A in Fig. 2) and Fig. 3(b) shows the dimensionless temperature variation for NTU = 20, $U = 0.1$, and $R = 1.0$ (Case B in Fig. 2). Notice in Case A that the entrained fluid is assumed to have no thermal mass and therefore in this limit the fluid temperature responds instantaneously to changes in the flow or changes in the regenerator temperature. The regenerator temperature fluctuates as the energy associated with the fluid flow is stored over a cycle; all of the heat transfer required for this energy storage must pass through the thermal resistance between the fluid and the regenerator and therefore there is a significant difference between θ_f and θ_r during the cycle. In Case B, the entrained fluid heat capacity is significant and therefore the fluid temperature does not respond instantaneously; rather a time lag exists between changes in the regenerator temperature and changes in the fluid temperature. Also, only a portion of the energy rejected by the flowing fluid must be stored in the regenerator; nominally half of this energy is stored in the entrained fluid when $R = 1$. As a result, the thermal energy that must be transferred between the fluid and the matrix is nominally 50% of its value in Case A and the temperature difference between θ_f and θ_r is reduced accordingly. The net result is that Case B exhibits better performance than Case A, as evidenced by the lower ineffectiveness in Fig. 2.

Notice in Fig. 2 that the behavior of the $R = 1.0$ curve at low NTU differs markedly at low NTU as compared to high NTU. The ineffectiveness actually is reduced with decreasing NTU. As NTU is reduced, more of the energy storage occurs in the fluid; the regenerator is thermally disconnected from the fluid whereas the fluid capacity of the entrained fluid is not. This effect is not seen for the $R = 0$ curve in which ineffectiveness monotonically decreases with increasing NTU and therefore must be directly related to the entrained fluid heat capacity.

Fig. 4(a) illustrates the dimensionless temperature as a function of dimensionless axial position for NTU = 1.0, $U = 0.1$, and $R = 0$ (Case C in Fig. 2) and Fig. 4(b) shows the dimensionless temperature profile for NTU = 1.0, $U = 0.1$, and $R = 1.0$ (Case D in Fig. 2). In Case C, the entrained fluid heat capacity is assumed to be zero which is consistent with a matrix that has no dead volume. For the low NTU case shown in Fig. 4(a), the fluid cannot communicate effectively with the matrix heat capacity and therefore experiences very little heat transfer as it passes through the regenerator in either direction. This situation is analogous to passing a large mass flow rate through a small pipe with very little surface area; the fluid temperature is changed very little over a period and therefore the ineffectiveness in this limit is large. The regenerator temperature changes slightly during the cycle. The fluid temperature changes instantaneously at the conclusion of the flow processes in the absence of entrained fluid heat capacity; at $t/\lambda = 1.0^-$, the end of the hot-to-cold flow process, the dimensionless fluid temperature goes from 1.0 at $x/L = 0$ to nominally 0.67 at $x/L = 1.0$. At $t/\lambda = 1.0^+$, the beginning of the cold-to-hot flow process, the dimensionless fluid temperature goes from 0.0 at $x/L = 1.0$ to nominally 0.33 at $x/L = 0$.

In Case D, the entrained fluid heat capacity is large relative to the fluid passing through the matrix. When $U = 0.1$ and $R = 1.0$, the capacity of the entrained fluid is $5\times$ the capacity of the flowing fluid. Said differently, the void volume of the matrix is approximately $5\times$ the volume of the flow that enters the matrix during the flow processes. As a result, the matrix stops acting like a conventional regenerator and instead acts as a stratified storage tank. A fluid temperature distribution forms that has a nearly constant shape and a sharp transition from hot to cold. The position of the temperature distribution oscillates axially during the cycle; during the hot-to-cold flow process, it moves towards the cold

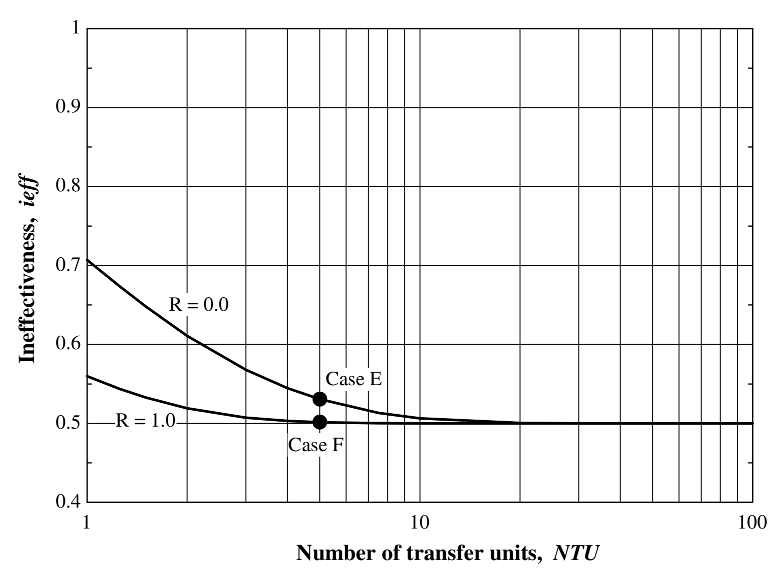

Fig. 5. Ineffectiveness as a function of NTU for $U = 2.0$, a regenerator in which the total heat capacity is half the capacity of the flowing fluid capacity with $R = 0.0$ (all capacity in the matrix) and $R = 1.0$ (capacity split equally between matrix and entrained fluid).

end. For the conditions considered in Fig. 4(b), the axial oscillation is nominally 20% of the length of the bed. During the cold-to-hot flow process, the temperature distribution moves back towards the hot end. In this limit, the ineffectiveness approaches zero as the number of transfer units drops and the regenerator heat capacity becomes further de-coupled from the process. The cold fluid is essentially stored in the bed during the cold-to-hot flow part of the process and then delivered again to the cold end during the hot-to-cold flow part of the process. The regenerator matrix is not well-coupled to the fluid and therefore the temperature distribution in the matrix material is essentially unchanging in time. It should be noted that this is not a practical operating condition for most regenerative systems as effects such as axial conduction, mixing, and dispersion would tend to eliminate the standing wave in favor of a more uniform temperature distribution. This behavior is referred to as "stratified" because it resembles the behavior expected for a stratified storage tank.

Fig. 5 illustrates the ineffectiveness as a function of number of transfer units for a high utilization, $U = 2.0$ for two values of R, $R = 0.0$ and $R = 1.0$, corresponding to two regenerators that have the same total heat capacity which is less than the heat capacity of the flowing fluid. Again, in the $R = 0$ case this heat capacity is entirely in the matrix whereas in the $R = 1.0$ case the heat capacity is split equally between the matrix and the entrained fluid.

Fig. 6(a) illustrates the dimensionless temperature as a function of dimensionless time for $\text{NTU} = 5.0$, $U = 2.0$, and $R = 0$ (Case E in Fig. 5) and Fig. 6(b) shows the dimensionless temperature variation for $\text{NTU} = 5.0$, $U = 2.0$, and $R = 1.0$ (Case F in Fig. 5). Notice that in either case, the fluctuation of the fluid temperature during a cycle is quite large due to the limited heat capacity. The performance of the regenerator is therefore fundamentally limited by the total heat capacity available in the regenerator; the distribution of the heat capacity between the matrix and entrained fluid does not affect this limit, as evidenced in Fig. 5 by the fact that the $U = 2.0$ curves collapse for $R = 0.0$ and $R = 1.0$. This behavior is referred to as "capacity-limited".

Figs. 3, 4 and 6 illustrate three basic behaviors that can describe a regenerator with entrained fluid heat capacity. The "stratified" behavior tends to occur at low NTU, low U, and high R where the heat capacity of the entrained fluid is large relative to the heat capacity of the flowing fluid and the heat capacity of the matrix is decoupled from the problem. In this limit of NTU going to zero, the ineffectiveness approaches 0. The "capacity-limited" behavior tends to occur at high U (>1), high NTU, and becomes more pronounced at higher values of R (although this behavior is also exhibited with $R = 0$) when the temperature variation of the fluid is

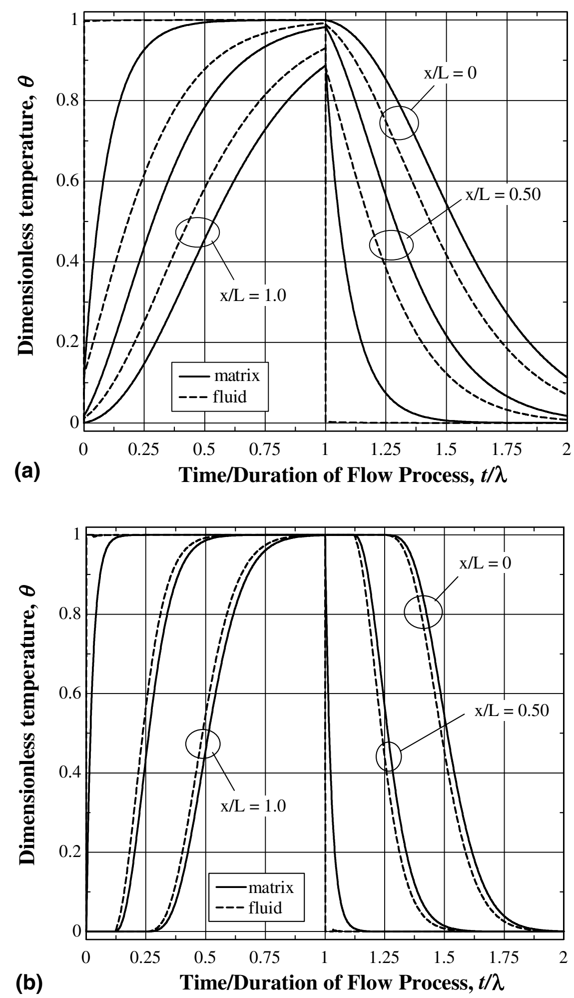

Fig. 6. Dimensionless temperature as a function of dimensionless time at several axial locations for (a) Case E: $\text{NTU} = 5.0$, $U = 2.0$, and $R = 0.0$, and (b) Case F: $\text{NTU} = 5.0$, $U = 2.0$, and $R = 1.0$.

limited by the total available heat capacity and therefore the ineffectiveness becomes independent of either NTU or R and instead depends only on U. Finally, there is the typical operating region associated with a regenerator, referred to as "NTU-limited" behavior which tends to occur at moderate to low values of R, high NTU, and low U. In this region, the available heat capacity is large relative to the heat capacity of the fluid and the fluid is in intimate contact with the regenerator matrix.

Fig. 7 illustrates the ineffectiveness as a function of NTU for several values of U and a fixed value of $R = 0.5$. In Fig. 7 it is possible to determine the points that delineate the three regimes of behavior that have been discussed. At high values of U, the curves asymptote to some fixed value of ineffectiveness; the transition between "NTU-limited" and "capacity-limited" behav-

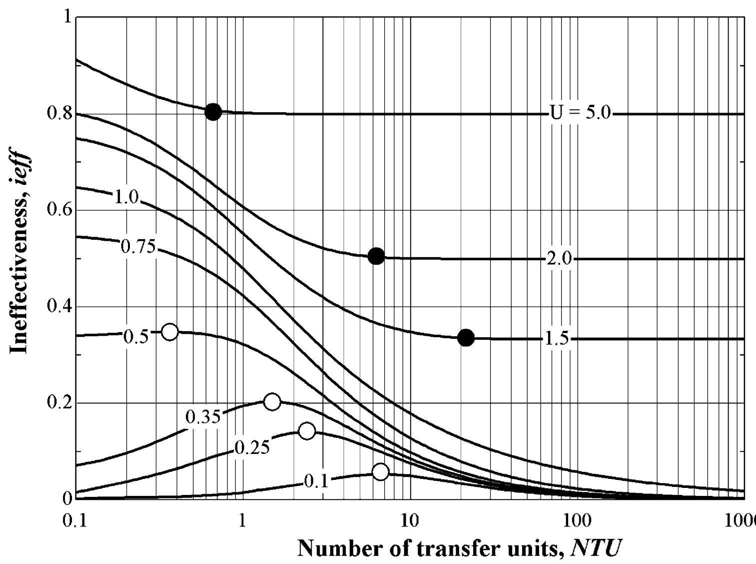

Fig. 7. Ineffectiveness as a function of NTU for $R = 0.5$ and various values of U. Note that the transition between "NTU-limited" and "capacity-limited" behavior is shown by the solid circles on the high U curves and the transition between "stratified" and "NTU-limited" behavior is shown by the open circles on the low U curves.

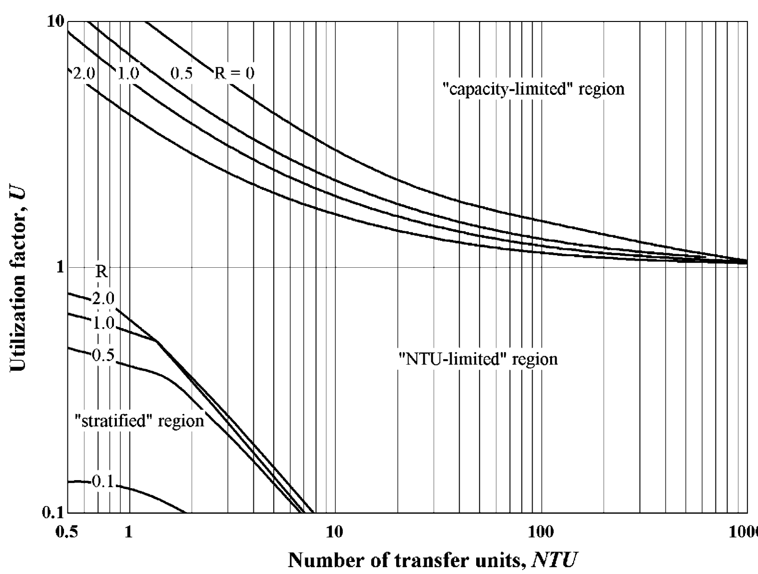

Fig. 8. Regions of "stratified", "capacity-limited", and "NTU-limited" behavior in the space of NTU and U for various values of R.

ior is shown by the solid symbols in Fig. 7. At low values of U, the curves exhibit a maximum at some low value of NTU. The transition between "stratified" and "NTU-limited" is shown by the open symbols in Fig. 7.

Fig. 8 illustrates the different regimes of behavior in the space of NTU and U for different values of R; for the $R = 0.5$ case, the curves shown in Fig. 8 are obtained by plotting the open and closed symbols shown in Fig. 7 in terms of their NTU and U values. The "stratified" behavior occurs in the lower left-hand corner of Fig. 8; the extent of this region grows with increasing R. There is no region of "stratified" behavior in the limit of $R = 0$. The "capacity-limited" behavior occurs in the upper right-hand corner of Fig. 8; the extent of this region also grows with increasing R although this behavior is exhibited even in the limit of $R = 0$.

The typical operating condition for a regenerator is $U < 1$ and $\mathrm{NTU} > 10$, which corresponds to the

"NTU-limited" region. This region is therefore of considerable, practical interest to the regenerator designer and the following section presents a technique whereby the performance enhancement associated with entrained fluid heat capacity can be accounted for using an augmented-NTU in the "NTU-limited" region.

6. Augmented-NTU approach

Fig. 9 illustrates the ineffectiveness as a function of NTU for $U = 0.3$ and several values of R. As previously discussed, increasing R tends to improve the performance of the regenerator and therefore, the use of an $R = 0$ solution for a matrix with a non-zero R will over-predict the ineffectiveness. Case G in Fig. 9 corresponds to $U = 0.3$, NTU = 40, and $R = 0.5$ and results in an ineffectiveness of 0.026. If the performance at this condition were evaluated in the $R = 0$ limit, corresponding to Case H ($U = 0.3$, NTU = 40, $R = 0$) in Fig. 9, then a much larger ineffectiveness would be predicted, nominally 0.054. The augmented-NTU technique can be used to approximately account for this effect by artificially increasing the NTU associated with the regenerator in order to account for the reduced matrix-to-fluid heat transfer that is required as R increases. The augmented-NTU is determined by finding the NTU with $R = 0$ that results in the same ineffectiveness predicted for the non-zero R condition; in Fig. 9, this augmented NTU operating point is shown as Case I ($U = 0.3$, NTU = 90.5, $R = 0$). Therefore, the augmented-NTU, referred to as NTU*, associated with $U = 0.3$, $R = 0.5$, and NTU = 40 is 90.5. This approach is analogous to the idea of using a pseudo-Stanton number or apparent heat transfer coefficient to account for particle internal conductivity or axial dispersion, as described by Jeffreson [12]. Notice that the range of NTU shown in Fig. 9 is restricted to the "NTU-limited" region and the augmented-NTU approach described in this section is likewise restricted to this region.

The augmented number of transfer units (NTU*) is defined as the number of transfer units that would give the same ineffectiveness with $R = 0$:

$$\mathrm{NTU}^* = \mathrm{NTU}(\mathrm{ieff}(\mathrm{NTU}, U, R), U, R = 0) \tag{43}$$

NTU* has the same functional dependence as the ineffectiveness:

$$\mathrm{NTU}^* = \mathrm{NTU}^*(\mathrm{NTU}, U, R) \tag{44}$$

Fig. 10 illustrates the NTU* for $U = 0.3$ as a function of NTU and the same values of R that were shown in Fig. 9. Note that the relationship between NTU* and NTU is essentially linear for any given value of R and U; these lines approximately pass through zero and therefore the augmented number of transfer units can be written as:

$$\mathrm{NTU}^* = \mathrm{AF}(R, U)\mathrm{NTU} \tag{45}$$

where AF is the slope of the line, referred to as the augmentation factor, which is in general a function of both R and U. The best fit lines for the various R values are also shown in Fig. 10.

Fig. 11 illustrates the augmentation factor as a function of R for various values of U. Notice that the aug-

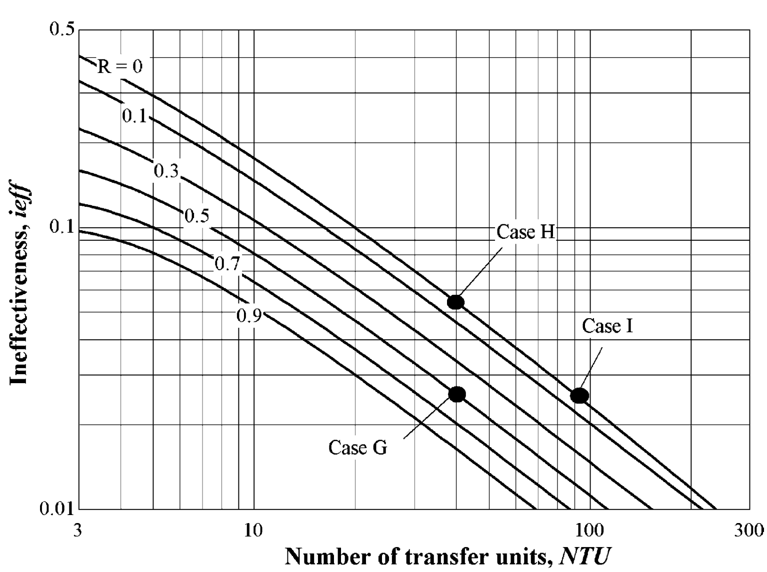

Fig. 9. Ineffectiveness as a function of NTU for $U = 0.3$ and various values of R.

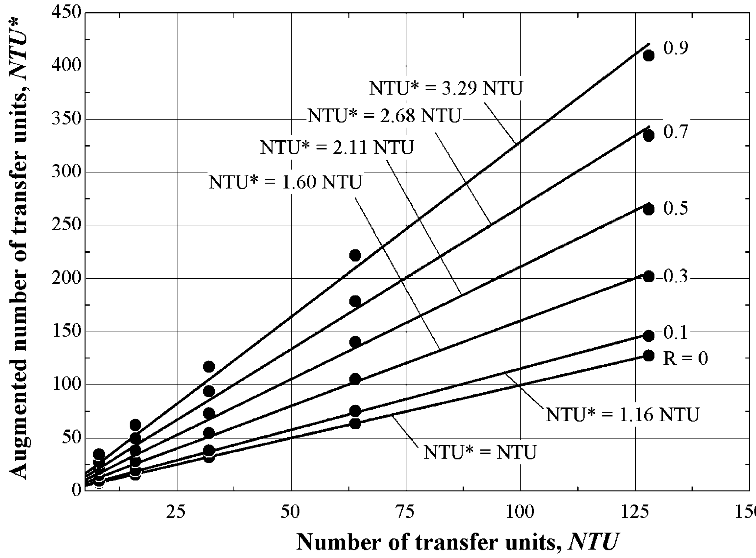

Fig. 10. Augmented-NTU as a function of NTU for $U = 1.0$ and various values of R. Notice that the variation is essentially linear and can be described by Eq. (45); the best fit lines are also shown.

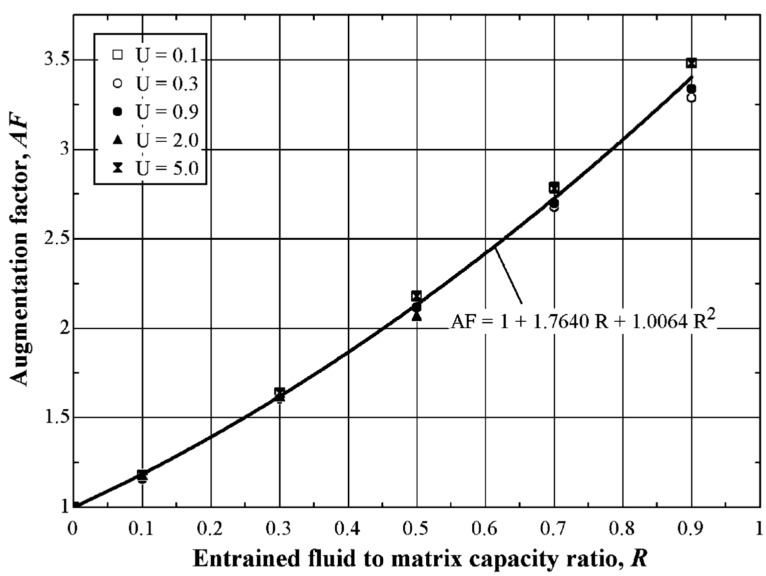

Fig. 11. Augmentation factor as a function of R for various values of U. The best-fit polynomial that described AF(R) is given by Eq. (46) and shown as the heavy line.

mentation factor is not a strong function of U provided that the range of U and NTU considered does not extend into the "capacity-limited" or "stratified" regions shown in Fig. 8. In the "NTU-limited" region, the augmentation factor is a function only of R. The best-fit polynomial to the augmentation factor is also shown in Fig. 11 and is given below:

$$\mathrm{AF} = 1 + 1.7640R + 1.0064R^2 \tag{46}$$

7. Conclusions

The effect of entrained fluid heat capacity is not typically considered in the analysis of regenerative heat exchangers. This paper describes a numerical model in which this effect is specifically analyzed. It is shown that the behavior of a regenerator with entrained fluid heat capacity can be divided qualitatively into three regimes.

1. A "stratified" regime in which the fluid flow has a small capacity relative to the entrained fluid heat capacity and the fluid is de-coupled thermally from the regenerator. In this limit, a standing wave exists that oscillates axially during the flow processes.
2. A "capacity-limited" regime in which the total capacity of the matrix and entrained fluid is small relative to the fluid flow capacity. In this limit, the performance of the matrix is limited by the available heat capacity and is independent of the distribution of this capacity or the number of transfer units.
3. An "NTU-limited" regime, which is typical of most regenerator operating conditions. In this regime, the performance of the regenerator is a function of the total available heat capacity, the thermal communication between the regenerator and the fluid, and the distribution of the total heat capacity between the entrained fluid and the matrix.

The "NTU-limited" regime is of the greatest practical interest to the regenerator designer and therefore the effect of the entrained fluid heat capacity in this region was investigated. It was found that it is always beneficial to have a larger fraction of the total heat capacity in the regenerator associated with the entrained fluid as compared with concentrated in the matrix material. This heat capacity is accessible to the flowing fluid without requiring a heat flow through the thermal resistance associated with the heat transfer coefficient between the fluid and the matrix material. In order to quantify this effect and correct for it, the concept of an augmented number of transfer units was introduced. The augmented NTU reflects the reduction in the fluid-to-matrix heat transfer that accompanies the increase in the entrained fluid heat capacity. It was found that the augmented-NTU was a linear function of NTU; the slope of this linear function is defined as the augmentation factor and depends on the entrained fluid to regenerator heat capacity ratio, R, but not the utilization factor, U. The augmentation factor is correlated with R in the "limited-NTU" region.

Acknowledgements

Financial support for this project was provided by the Air-Conditioning and Refrigeration Technology Institute (ARTI) under contract 21-CR/612-10075. The discussions with personnel at Astronautics Corporation, in particular A. Sternberg, were extremely helpful and are gratefully acknowledged.

References

[1] W. Nusselt, Die Theorie des Winderhitzers, VDI-Zeitung 71 (1927) 85–91.
[2] A. Hill, A.J. Wilmott, Accurate and rapid thermal regenerator calculations, Int. J. Heat Mass Transfer 32 (1989) 465–476.
[3] D.R. Atthey, An approximate thermal analysis for a regenerative heat exchanger, Int. J. Heat Mass Transfer 31 (1988) 1431–1444.
[4] G.D. Bahnke, C.P. Howard, The effect of longitudinal heat conduction on periodic flow heat exchanger performance, ASME J. Eng. Power 86 (1964) 105–120.
[5] C.M. Shen, W.M. Worek, The effect of wall conduction on the performance of regenerative heat exchangers, Energy 17 (1992) 1199–1213.
[6] H. Klein, G. Eigenberger, Approximate solutions for metallic regenerative heat exchangers, Int. J. Heat Mass Transfer 44 (2001) 3553–3563.
[7] K.A. Gshneidner Jr., V.K. Pecharsky, Magnetic refrigeration material, J. Appl. Phys. 85 (1999) 5365–5368.
[8] X. Bohigas, E. Molins, A. Roig, J. Tejada, X.X. Zhang, Room-temperature magnetic refrigerator using permanent magnets, IEEE Trans. Magn. 36 (2000) 538–544.
[9] B.F. Yu, Q. Gao, B. Zhang, X.Z. Meng, Z. Chen, Review on research of room temperature magnetic refrigeration, Int. J. Refrig. 26 (2003) 622–636.
[10] A.J. Willmott, C. Hinchcliffe, The effect of gas heat storage on regenerator calculations, Int. J. Heat Mass Transfer 19 (1976) 821–826.
[11] D.E. Daney, R. Radebaugh, Non-ideal regenerator performance—the effect of void volume fluid heat capacity, Cryogenics 24 (1984) 499–501.
[12] C.P. Jeffreson, Prediction of breakthrough curves in packed beds: I. Applicability of single parameter models, AIChE J. 18 (1972) 409–416.
[13] R.A. Ackerman, Cryogenic Regenerative Heat Exchangers, Plenum Press, New York, 1997, pp. 61–78.
[14] G.D. Dragutinovic, B.S. Baclic, Operation of Counterflow Regenerators, Computational Mechanics Publications, Billerica, 1998, pp. 100–101.